Theoretical and Experimental Analysis of Ammonia Ionic Clusters Produced by ^{252}Cf Fragment Impact on an NH_3 Ice Target

F. A. Fernandez-Lima,[†] C. R. Ponciano,[†] M. A. Chaer Nascimento,[‡] and E. F. da Silveira*[,†]

Physics Department, Pontifícia Universidade Católica, Rua Marques de São Vicente 225, 22543-970 Rio de Janeiro, Brazil, and Instituto de Química, Universidade Federal do Rio de Janeiro, Rio de Janeiro, Brazil

Received: March 30, 2006; In Final Form: June 16, 2006

Positive and negatively charged ammonia clusters produced by the impact of ^{252}Cf fission fragments (FF) on an NH_3 ice target have been examined theoretical and experimentally. The ammonia clusters generated by ^{252}Cf FF show an exponential dependence of the cluster population on its mass, and the desorption yields for the positive $(NH_3)_nNH_4^+$ clusters are 1 order of magnitude higher than those for the negative $(NH_3)_nNH_2^-$ clusters. The experimental population analysis of $(NH_3)_nNH_4^+$ ($n = 0-18$) and $(NH_3)_nNH_2^-$ ($n = 0-8$) cluster series show a special stability at $n = 4$ and 16 and $n = 2$, 4, and 6, respectively. DFT/B3LYP calculations of the $(NH_3)_{0-8}NH_4^+$ clusters show that the structures of the more stable conformers follow a clear pattern: each additional NH_3 group makes a new hydrogen bond with one of the hydrogen atoms of an NH_3 unit already bound to the NH_4^+ core. For the $(NH_3)_{0-8}NH_2^-$ clusters, the DFT/B3LYP calculations show that, within the calculation error, the more stable conformers follow a clear pattern for $n = 1-6$: each additional NH_3 group makes a new hydrogen bond to the NH_2^- core. For $n = 7$ and 8, the additional NH_3 groups bind to other NH_3 groups, probably because of the saturation of the NH_2^- core. Similar results were obtained at the MP2 level of calculation. A stability analysis was performed using the commonly defined stability function $E_{n-1} + E_{n+1} - 2E_n$, where E is the total energy of the cluster, including the zero point correction energy ($E = E_t + \mathrm{ZPE}$). The trend on the relative stability of the clusters presents an excellent agreement with the distribution of experimental cluster abundances. Moreover, the stability analysis predicts that the $(NH_3)_4NH_4^+$ and the even negative clusters [$(NH_3)_nNH_2^-$, $n = 2$, 4, and 6] should be the most stable ones, in perfect agreement with the experimental results.

1. Introduction

There is considerable experimental and theoretical interest in the study of molecular clusters in the gas phase and in the solid state. Clusters are of fundamental interest both due to their own intrinsic properties and because of the central position that they occupy between molecular and condensed matter science. The study of how the geometric and electronic structures of the clusters as well as their chemical and physical properties change as the size of the cluster increases is also of great fundamental interest. Since many cluster properties (e.g., cluster geometries, binding energies, and energy barriers) are not easily measured directly from experiment, theoretical models and computational methods have been very useful in helping to interpret spectroscopic and mass spectrometric (MS) data.[1−6]

In cluster experiments, the extent of clustering depends on many factors: cluster nucleation, cluster growth, cluster temperature, cluster cooling, and distribution of cluster sizes. Many experiments involving clusters rely on the possibility of separating them according to their mass. To do this, one generally needs to ionize the clusters so that mass selection can be accomplished by deflecting the clusters in a magnetic or electric field. Among the most basic probes for cluster ion structure and dynamics are mass spectroscopy, photoelectron spectroscopy, photofragment spectroscopy, and several relatively new ultrafast pump−probe techniques.

In recent years, there have been a large number of accurate theoretical as well as experimental investigations on hydrogen-bonded molecular clusters of polar molecules, especially water and ammonia containing clusters.[7−21] The generation of positively charged ammonia clusters has been performed using several ionization techniques, such as multiphoton ionization (MPI),[22−24] single photon ionization,[25] electron impact ionization (EII),[26−28] and ultrafast pump−probe techniques.[29−31] Several positively charged ammonia cluster series have been observed experimentally: $(NH_3)_nNH_2^+$, $(NH_3)_nNH_3^+$, $(NH_3)_nNH_5^+$, and $(NH_3)_nNH_4^+$; the last one is the predominant. The generation of negatively charged ammonia clusters $(NH_3)_{n=0-2}NH_2^-$ has only been reported using photoelectron spectroscopy.[32]

Recently, the generation of ammonia cluster ions (positive and negative) has been performed via the impact of highly energetic and highly charged fission fragments (FF) from a ^{252}Cf source on the NH_3 ice surface at controlled temperatures.[33] Differently from the previous ionization techniques, besides the positive ammonia cluster series ($(NH_3)_nNH_{2-5}^+$), negatively charge ammonia clusters ($(NH_3)_{1-8}NH_2^-$) were also observed. This last process, electronically induced sputtering on low-temperature condensed-gas solids (ices) [see, e.g., refs 34−38], is important for understanding atmospheres, cometary surfaces, and outer-solar-system bodies.[39−41]

On the theoretical side, the first attempts at describing the metastable decomposition of cluster ions and at determining

* Corresponding author. Telephone: 55-21-35271272. Fax: 55-21-35271040. E-mail: enio@fis.puc-rio.br.
[†] Pontifícia Universidade Católica.
[‡] Universidade Federal do Rio de Janeiro.

10.1021/jp0619944 CCC: $33.50
Published on Web 07/29/2006

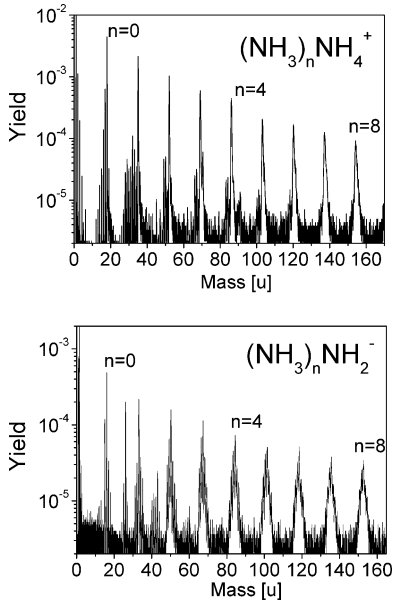

Figure 1. TOF mass spectra of $(NH_3)_nNH_4^+$ and $(NH_3)_nNH_2^-$ clusters produced by ^{252}Cf FF impact.

cluster ion binding energies used several statistical models.[42−45] Later on, with the advent of predictive ab initio methods, cluster ions were investigated with several different methodologies including accurate ab initio methods that include electron correlation. Since the early works of Pullman et al.[46] and Hirao et al.,[47] ab initio calculations of $(NH_3)_nNH_4^+$ clusters have been extensively performed using the Hartree−Fock method (HF),[28,48] the Møller−Plesset (MP) perturbation theory,[28,49−51] the coupled cluster methods (CC),[49,51,52] and the density functional theory (DFT) with extended basis sets.[48,49,51]

Although studies on positively charged ammonia clusters have been reported, a comprehensive and accurate theoretical calculation of negatively charged ammonia clusters is missing. Motivated by this, we present in this paper an experimental population analysis of $(NH_3)_nNH_4^+$ ($n = 0-18$) and $(NH_3)_nNH_2^-$ ($n = 0-8$) cluster series produced by a ^{252}Cf FF impact onto an NH_3 ice target. In particular, we are interested in establishing if the cluster stability could be directly related to the relative cluster populations in the mass spectra. To accomplish that, we searched systematically for the more stable conformers of $(NH_3)_nNH_4^+$ and $(NH_3)_nNH_2^-$ cluster series using density functional theory (DFT) at the B3LYP level of calculation with extended basis set. The negative clusters were also treated at the MP2 level, with the same basis set.

2. Experimental Results

The experimental details of ^{252}Cf plasma desorption mass spectrometry (PDMS) can be found elsewhere.[33−37,53] Briefly, an NH_3 ice target was grown by condensation of an NH_3 gas over an Au substrate at controlled low temperature. Fission fragments from a ^{252}Cf source are impacted onto the NH_3 ice target inducing desorption of positive and negative ions, as well as neutral particles, at high vacuum conditions (10^{-9} mbar). The desorbed ions are accelerated by the extraction field toward the drift region and are detected by the secondary ion detector. Negatively and positively charged ions are measured sequentially by reversing the high voltage polarity. Mass analysis is performed by the time-of-flight (TOF) technique. In Figure 1, TOF mass spectra of $(NH_3)_nNH_4^+$ and $(NH_3)_nNH_2^-$ clusters produced by ^{252}Cf FF impact are presented. A correction has been applied to take into account that the detection efficiency

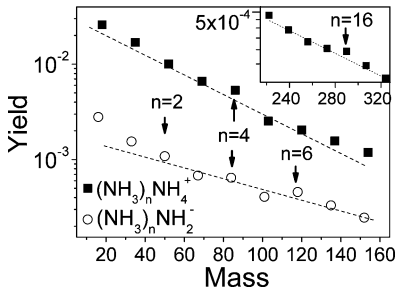

Figure 2. Semilogarithmic plot for FF desorption-induced ammonia ion cluster yields. The second "magic number" for the protonated ammonia is shown in the inset.

of the ionized clusters varies smoothly and monotonically across the mass range. A typical mass-resolution power in the current spectra is about $m/\Delta m \sim 200$ in the worst case (mass 155 u). In the low mass region (below 110 u or $n = 5$), the principal $(NH_3)_nNH_4^+$ and $(NH_3)_nNH_2^-$ peaks are completely separated from their satellite peaks. The satellite peaks are at least 1 order of magnitude lower than their principal peaks. For $n > 5$, the dominant and the satellite signals are no longer resolved and a peak decomposition was performed assuming that their relative yields are about the same as in the lower mass region. A semilogarithmic plot for desorption yields (i.e., number of desorbed ions per FF impact) of the ammonia cluster ions is shown in Figure 2.

3. Theoretical Results

Theoretical calculations have been performed with the purpose of determining the most stable structures of the ammonia clusters and to investigate if the clusters' stability could be directly related to their relative cluster populations in the MS spectra.

Ammonia cluster structures were calculated using DFT at the B3LYP/6-31G** level for the positively charged species and at the B3LYP/6-31G**++ for the negatively charged clusters, using the Jaguar 5.5 and Jaguar 6.0 programs.[54] The strategy adopted for the different kinds of clusters took into consideration the nature of the dominant forces stabilizing the clusters and the character (diffuseness) of the wave functions. For charged clusters, the electrostatic forces are dominant, and these can be well described with the B3LYP functional. However, the choice of the basis set must take into account the nature of the systems. For the cationic clusters the electronic density is more contracted, while for the anionic ones it is more diffuse. Thus, for the anionic clusters we used the B3LYP functional with diffuse basis functions, while for the cationic clusters no diffuse functions are needed. The negative clusters were also treated at the MP2 level, since DFT calculations of negative ions are more susceptible to errors[55] due to the fact that, for the presently available functionals, the exchange energy does not exactly cancel the Coulombic self-interaction. The basis set superposition error (BSSE) was found to be on the order of 0.02 eV. The accuracy of the B3LYP functional is known to be on the order of ~3 kcal/mol, meaning that conformers differing by less than that amount cannot be distinguished at this level of calculation. No symmetry restrictions have been imposed in the process of geometry optimization.

$(NH_3)_nNH_4^+$. The infrared spectra of protonated ammonia clusters $[(NH_3)_nH]^+$ shows that there are strong absorption bands due to a central ammonium NH_4^+ cation and weaker bands due to the remaining neutral ammonia clusters, so that the cluster should be written as $(NH_3)_{n-1}NH_4^+$ instead of $(NH_3)_nH^+$, with a central ammonium ion solvated by neutral ammonia mol-

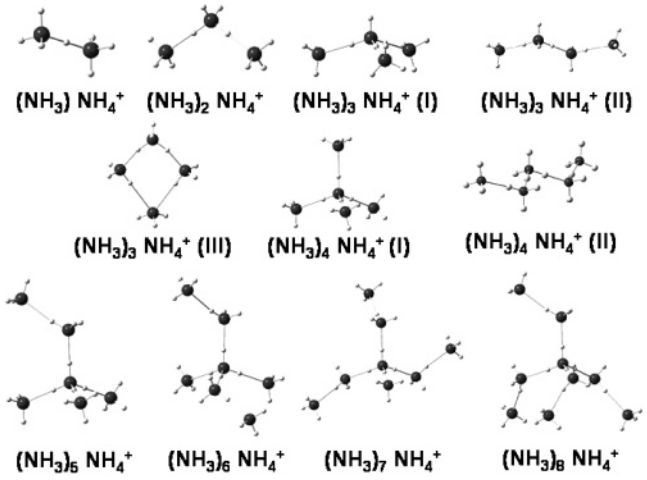

Figure 3. Optimized geometries of $(NH_3)_nNH_4^+$ clusters at the B3LYP/6-31G** level of calculation.

ecules.[5,28] Such a structure is analogous to that found for protonated water clusters.[5,28] A strong red shift of the N−H stretching modes of the NH_4^+ core is observed, though the shifts on the vibrations of the outer NH_3 molecules are much smaller.[56]

In Figure 3, the optimized geometries for some of the $(NH_3)_n$-NH_4^+ clusters are shown. A vibrational analysis was performed for all the clusters shown in Table 1 at the level of calculation employed, and all frequencies were found to be real, indicating that the optimized structures correspond to true minima in the potential energy hypersurfaces.

For $n = 1$ and 2, the clusters seem to exhibit only one stable structure. However, for $n = 3$, three possible conformers are found. The energy analysis shows that the $(NH_3)_3NH_4^+$ (I) conformer is the most stable one, with energy differences of 4.77 and 6.8 kcal/mol relative to the II and III conformers, respectively. For $n = 4$, two conformers are found, with $(NH_3)_4$-NH_4^+ (I) being more stable than $(NH_3)_4NH_4^+$ (II) by 7.87 kcal/mol. For $n > 5$, we found no evidence for the existence of more than one stable conformer.

It may be noted that the "linear" species are typically higher in energy than their more stable and relatively more compact "cyclic" counterparts. The structures of the more stable clusters follow a clear pattern with each additional NH_3 group making a new hydrogen bond with one of the hydrogen atoms of an NH_3 unit already bound to the NH_4^+ core. The general structure of the more stable clusters does not differ substantially from the previously reported structures,[46−52] computed at different levels of calculation, but limited to clusters with $n \leq 5$. Although the calculations by Nakai et al.[48] used a larger basis set, no isomers have been reported for any members of the cluster series. On the other hand, we paid special attention to the possibility of isomers because they could all contribute to the intensity of a given mass peak in the mass spectra.

$(NH_3)_nNH_2^-$. No report of negatively charged ammonia clusters formed by the loss of a proton from neutral ammonia clusters was found in the literature. On the other hand, negatively charged ammonia clusters $(NH_3)_n^-$ have been observed only for $n \geq 34$, possibly because for these sizes of clusters the electron solvation is already large enough to overcome the instability of the surface electronic states of the negatively charged ammonia clusters.[1,5]

In Figure 4, the geometries of $(NH_3)_nNH_2^-$ clusters optimized at the B3LYP/6-31G**++ level of calculation are shown. Very similar results were obtained at the MP2 level of calculation with the same basis set. A vibrational analysis was performed for all the clusters shown in Table 2, and all frequencies were found to be real, indicating that the optimized structures correspond to true minima in the potential energy hypersurfaces.

For $n = 1$ and 2 only one stable structure was found. However for $n = 3$ and 4, two conformers are possible: $(NH_3)_3NH_2^-$ (I), $(NH_3)_3NH_2^-$ (II), and $(NH_3)_4NH_2^-$ (I), $(NH_3)_4NH_2^-$ (II), respectively. In both cases, the energy difference between the conformers is smaller than the accuracy of the level of the calculation employed (0.85 and 0.21 kcal/mol, respectively). Therefore, one cannot tell which structure is the most stable. For $n > 5$, we found no evidence for the existence of more than one stable conformer. It may be noted that, within the calculation error, the lowest energy conformers follow a clear pattern for $n = 1-6$: each additional NH_3 group makes a new hydrogen bond to the NH_2^- core. For $n = 7$ and 8, the additional NH_3 group must bind to two other NH_3 groups, because of the saturation of the NH_2^- core. Larger clusters ($n > 6$) necessarily have to be formed by the addition of NH_3 groups to the NH_3 group terminals, opening a new shell.

4. Discussion

If there is any inherent stability associated with a given number of atoms in a cluster, then, all other factors being equal, this will give rise to a greater abundance of this cluster and a large peak in MS intensity (i.e., a "magic" number), relative to similarly sized clusters.

When clusters are generated by FF[33−38] and by multiphoton ionization,[22−24] an exponential dependence of the cluster population on its mass has been observed as a general trend. The yield distributions can be fitted quite well by an exponential function for the $n < 8$ interval: $Y = Y_0 e^{-k_m m(n)}$, where $m(n)$ is the mass of the cluster with size n (nuclearity). The slope parameter k_m is more adequate for secondary ion dynamics analysis,[57] giving $k_m(NH_4^+) = 0.024$ (and 0.039) and $k_m(NH_2^-) = 0.014$ for the FF (and MPI) generated clusters. Such exponential behavior, characteristic of these two processes of cluster production, was subtracted from the experimental data to search for fluctuations generated by the cluster stabilities. The yield deviations in the populations of $(NH_3)_nNH_4^+$ clusters obtained from three different experiments (MPI, EII, and FF) are shown in Figure 5a. They all indicate that the cluster with $n = 4$ is especially stable. Moreover, the yield deviations in the population of $(NH_3)_nNH_2^-$ clusters obtained in the present experiment (FF) indicate a special stability for the even clusters, i.e., for $n = 2$, 4, and 6 (Figure 5b).

Interpretation of mass spectral intensities and magic numbers is not straightforward, and a proper description of the cluster formation requires a dynamic approach. On the other hand, due to the complexity of a dynamic approach, it would be nice to have a simpler way of trying to understand the relative abundances of the clusters produced in a given experiment. One possibility would be the use of the cluster stability as a criterion to determine its relative abundance. The time scale of the TOF experiment is on the order of 10^{-6} s, while the time elapsed since the ionic cluster formation and its reorganization and fragmentation through unimolecular processes is on the order of $10^{-14}-10^{-13}$ s.[25] Therefore, it seems quite reasonable to assume that the species being detected are the thermodynamically more stable ones. Under this assumption one could then try to correlate the cluster population in the mass spectra with their relative stability.

The cluster stability can be related to two quantities: the binding energy (E_b, as defined below) and the cluster geometry (size of the solvation shell), which are of course closely related.

TABLE 1: Theoretical Results for the Clustering of Ammonia about an NH_4^+ Cation at the B3LYP/6-31G Level of Calculation, Compared to Other Theoretical Results[a]**

cluster	point group	E_T + ZPE [eV] DFT	E_b [eV] DFT	NH_4^+ core charge DFT
NH_4^+	T_d	−1547.153		1.00
$(NH_3)NH_4^+$	C_{3v}	−3086.710	1.464 (1.34)	0.79
$(NH_3)_2NH_4^+$	C_{2v}	−4625.637	0.836 (1.08)	0.73
$(NH_3)_3NH_4^+$ (I)	C_{3v}	−6164.469	0.740 (0.88)	0.66
$(NH_3)_3NH_4^+$ (II)	C_1	−6164.262	0.533	0.72
$(NH_3)_3NH_4^+$ (III)	C_1	−6164.175	0.445	0.72
$(NH_3)_4NH_4^+$ (I)	T_d	−7703.161	0.599 (0.73)	0.65
$(NH_3)_4NH_4^+$ (II)	C_{2v}	−7702.820	0.258	0.71
$(NH_3)_5NH_4^+$	C_s	−9241.627	0.374 (0.45)	0.61
$(NH_3)_6NH_4^+$	C_1	−10780.075	0.355 (0.44)	0.58
$(NH_3)_7NH_4^+$	C_1	−12318.530	0.363 (0.43)	0.54
$(NH_3)_8NH_4^+$	C_1	−13856.905	0.282 (0.42)	0.49

[a] Values in parentheses are from ref 48.

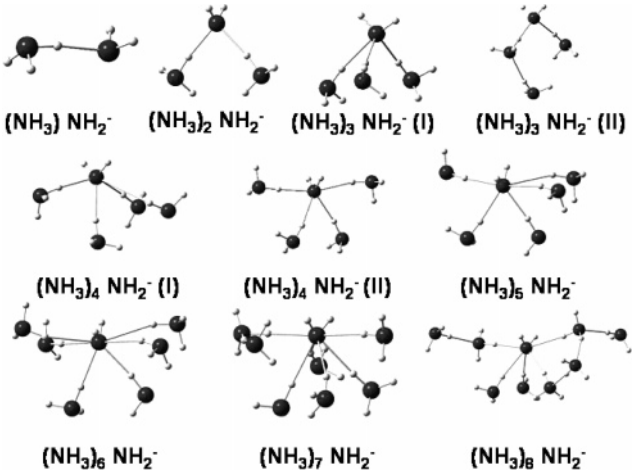

Figure 4. Optimized geometries of $(NH_3)_nNH_2^-$ clusters at the B3LYP/6-31G**++ level of calculation.

Figure 6 shows the binding energy as function of the cluster number for protonated and deprotonated ammonia clusters. The binding energies were calculated considering reactions 1 and 2 for the positively and negatively charged clusters, respectively:

$$(NH_3)_nNH_4^+ \rightarrow (NH_3) + (NH_3)_{n-1}NH_4^+ \quad (1)$$

$$(NH_3)_nNH_2^- \rightarrow (NH_3) + (NH_3)_{n-1}NH_2^- \quad (2)$$

For the $(NH_3)_nNH_4^+$ clusters, the binding energies are compared with previously reported experimental[22−24] (Figure 6a) and theoretical data[48−52] (Table 1). The comparison with experimental data is not straightforward because the data in refs 22−24 are not absolute values. They were calculated using the Engelking[42] and Klots[44,45] models, which have an independent variable that accounts for the intensity. Therefore, to compare them to our absolute results, the data from refs 22−24 were renormalized to our absolute value for $n = 7$. From Figure 6a one can see that the renormalized data,[22−24] the results of the present calculations, and also the results of Nakai et al.[48] follow the same tendency.

The calculated binding energies for the $(NH_3)_nNH_2^-$ clusters are shown in Table 2 and Figure 6b. Experimental binding energies, also shown in Table 2, were only found for $(NH_3)_{n=0-2}NH_2^-$ [32] and are in good agreement with the theoretical results. The binding in these clusters is essentially due to electrostatic forces. The NH_2^- negative core polarizes the NH_3 neutral units, resulting in a net attractive force that binds the units to the central core. In principle, the closer the NH_3 unit from the core, the stronger would be the attractive force. However, as the number of NH_3 units increases, steric effects start to play a role in determining how far from the central core these units can be. For $n = 8$, due to steric effects, the NH_3 units are farther apart than in the $n = 6$ and 7 clusters. On the other hand, for $n = 8$ the central core has the smallest negative charge among all the clusters, meaning that the negative charge of the cluster is spread over several NH_3 units, which can now act as new polarization centers for the outer NH_3 units. Thus, the larger binding energy predicted for the $n = 8$ cluster may be due to a combination of attraction of the central NH_2^- core plus mutual polarization among the ligands.

The stability analysis was performed using the commonly defined stability function $E_{n-1} + E_{n+1} - 2E_n$, where E is the total energy of the cluster, including the zero point correction energy ($E = E_t$ + ZPE). The trend of the stability analysis presents an excellent agreement with the distribution of experimental cluster abundances, showing the $n = 4$ for $(NH_3)_nNH_4^+$ and the even clusters ($n = 2$, 4, and 6) for the $(NH_3)_nNH_2^-$ as the most stable ones, in perfect agreement with the experimental results (see Figure 2).

The relative stability of the clusters will be a function of the charge stabilization provided by the NH_3 ligands and of the arrangement of these ligands around the central core to minimize the steric repulsion among them. From Figure 3 it is clear that for $n = 4$ one has the largest number of NH_3 units directly bound to the NH_4^+ core and in a tetrahedral arrangement providing the lowest steric repulsion among the ligands. Also, from Figure 4 it is clear that, for n up to 7, the even clusters, or at least one of their isomers, have all the ligands directly attached to the N atom of the NH_2^- core and their NH_3 units are farther apart than in their odd ($n + 1$) or ($n - 1$) neighbors. Thus, for the positive clusters $n = 4$ is the most stable one, and for the negative ones the most stable are the even $n = 2$, 4, and 6 clusters.

Figure 7 shows the distances from each atom to the center of mass for the protonated and deprotonated ammonia clusters. In the case of $(NH_3)_nNH_4^+$ clusters, the first solvation shell is completed at $n = 4$, and further additions of NH_3 molecules will open the second solvation shell, with the additional NH_3 molecules being attached to the terminal hydrogen atoms of the first solvation shell. The second solvation shell should be completed at $n = 16$, when the third solvation shell will start to be filled, probably according to the same mechanism. This also agrees with the experimental abundance observed (see inset of Figure 2) and with the previously reported theoretical data.[48−52] The stability analysis that would confirm $n = 16$ as the second magic number for the protonated clusters was not

TABLE 2: Theoretical Results for the Clustering of Ammonia about an NH_2^- Anion at the B3LYP/6-31G++ Level of Calculation, Compared to MP2/6-31G**++ Level of Calculation and to Available Experimental Results[a]**

cluster	point group	E_T + ZPE [eV] DFT	E_T [eV] MP2	E_b [eV] DFT	E_b [eV] MP2	NH_2^- core charge DFT
NH_2^-	C_{2v}	−1520.893	−1516.495			−1.00
$(NH_3)NH_2^-$	C_s	−3059.852	−3051.396	0.614 (0.54)	0.426	−1.00
$(NH_3)_2NH_2^-$	C_{2v}	−4598.702	−4586.549	0.505 (0.46)	0.678	−0.96
$(NH_3)_3NH_2^-$ (I)	C_1	−6137.339	−6121.379	0.307	0.355	−0.94
$(NH_3)_3NH_2^-$ (II)	C_1	−6137.301	−6121.115	0.270	0.090	−0.83
$(NH_3)_4NH_2^-$ (I)	C_1	−7675.923	−7656.153	0.239	0.299	−0.76
$(NH_3)_4NH_2^-$ (II)	C_1	−7675.932	−7656.007	0.248	0.152	−0.78
$(NH_3)_5NH_2^-$	C_1	−9214.422	−9190.879	0.154	0.397	−0.63
$(NH_3)_6NH_2^-$	C_1	−10752.937	−10725.644	0.170	0.289	−0.80
$(NH_3)_7NH_2^-$	C_1	−12291.460	−12260.410	0.178	0.292	−0.75
$(NH_3)_8NH_2^-$	C_1	−13830.262	−13795.185	0.457	0.299	−0.59

[a] Values in parentheses are from ref 32.

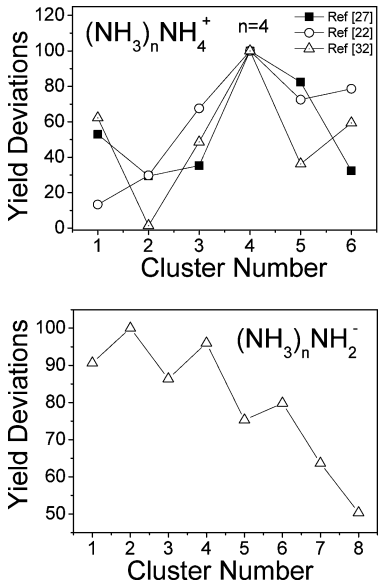

Figure 5. Yield deviations on the cluster population for positive (a, top) and negative (b, bottom) ammonia clusters. For positive ions, the yields obtained from three different cluster production sources are compared. All the results are normalized to $n = 4$ for the positive ions and $n = 2$ for the negative ions.

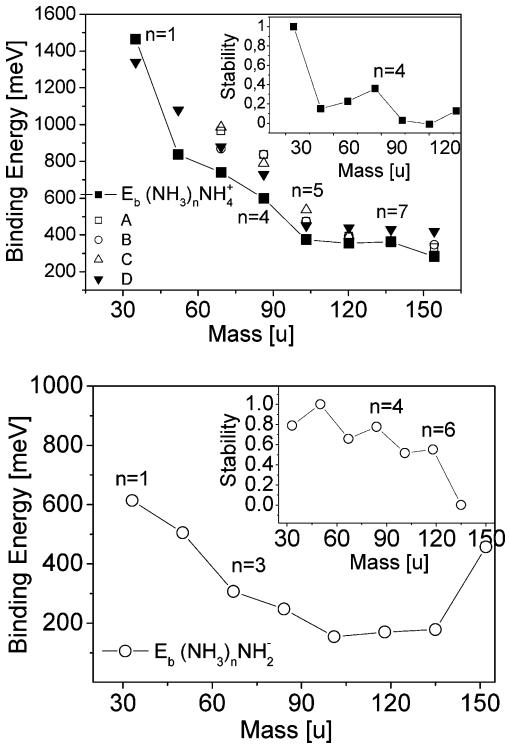

Figure 6. Calculated binding energies as function of cluster number for (a, top) protonated (positive ions) and (b, bottom) deprotonated (negative ions) ammonia clusters, compared to other results (A, B, and C from refs 22−24 and D from ref 48). The insets shown the respective stability functions, normalized to $n = 1$ and $n = 2$ for the protonated and deprotonated clusters, respectively.

performed because it would be extremely time-consuming. However, the structure of the solvation shells strongly suggests $n = 16$ as the second magic number for the protonated clusters.

Figure 8 shows the charges at the NH_4^+ and NH_2^- cores computed by fitting of the electrostatic potential using the CHelpG algorithm.[58] In this figure only the charges for the most stable conformers are plotted. The NH_4^+ core charge decreases as a function of the cluster size (Figure 8). Nevertheless, more than 50% percent of the charge (+1) is located at the ion core. When more than one stable conformer exists, comparison of the isomer core charges reveals that the less stable structures present higher charges. Thus, the preferential attachment of NH_3 units to the charged core would stabilize the charged core by spreading its charge among the attached units, enforcing at the same time the tetrahedral-like structure of the $(NH_3)_nNH_4^+$ clusters.

In the case of $(NH_3)_nNH_2^-$ clusters, the first solvation shell seems to be completed at $n = 6$, and further additions of NH_3 molecules will open the second solvation shell. Differently from the case of the protonated clusters, the first solvation shell is filled by attaching one hydrogen atom of the NH_3 molecule to the nitrogen atom of the NH_2^- anion ($n = 1-6$). This is understandable because nitrogen is more electronegative than hydrogen and the excess of negative charge will be concentrated on the N atom of the negative core. This charge density in excess around the nitrogen atom of the core is also more diffuse and more easily polarizable than the density along the covalent NH bonds. Thus, as long as the core retains most of the negative charge in excess, the number of NH_3 units that can be directly attached to the nitrogen atom of the core will be essentially defined by steric repulsion among the NH_3 ligands. For $n > 6$, to avoid steric hindrance, the additional NH_3 groups would have to bind to the N atom of the central core from the top, but that would be unfavorable because of the bad interaction with the NH bonds from the core. Thus, for $n = 7$, the extra NH_3 unit will have to bind to one of the NH_3 units already bound directly the core, opening a new shell. The structure of the second solvation shell suggests that it would be also completed at $n = 6$, when each of the NH_3 units of the first shell would be bound to an additional NH_3 unit. Steric effects should most probably

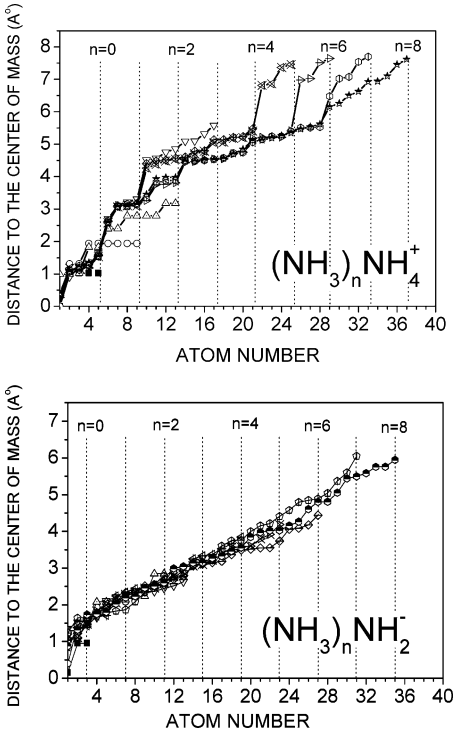

Figure 7. Variation of the distance from each atom to the center of mass for (a, top) $(NH_3)_nNH_4^+$ ($n = 0-8$) and (b, bottom) $(NH_3)_nNH_2^-$ ($n = 0-8$) clusters.

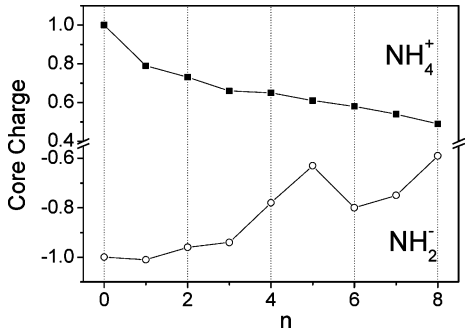

Figure 8. NH_4^+ and NH_2^- core charge as a function of cluster size ($n = 0-8$).

prevent the binding of more than one NH_3 unit to any of the NH_3 groups of the first shell.

The NH_2^- core charge increases as a function of the cluster size (Figure 8). Analogous to the positive clusters, more than 50% percent of the charge (-1) is located at the ion core. The decrease in the core charge observed at $n = 6$ is probably related to the fact that this structure presents the higher number of NH_3 units attached to the NH_2^- ion core. The saturation of NH_2^- ion core leads to the opening of the second shell, as discussed above.

The binding energies for the neutral ammonia clusters have been calculated to be much smaller[59] than the ones for the charged clusters presented in Tables 1 and 2. This is understandable in terms of the dominant forces holding the NH_3 units in the charged and neutral clusters. While the charged clusters are dominated by electrostatic forces, the neutral ones are held together by much weaker dispersion forces. Therefore, it would be reasonable to assume that the clustering process started by the impact of FF of ^{252}Cf on ice targets should involve preferentially the addition of NH_3 neutral units to charged fragments other than the addition of small charged fragments to neutral $(NH_3)_n$ clusters.

5. Conclusions

Positive and negatively charged ammonia clusters produced by the impact of ^{252}Cf fission fragments on an NH_3 ice target have been examined theoretically and experimentally.

The ammonia clusters generated by ^{252}Cf FF show an exponential dependence of the cluster population on its mass, and the desorption yields for the positive $(NH_3)_nNH_4^+$ clusters are 1 order of magnitude higher than those for the negative $(NH_3)_nNH_2^-$ clusters.

The experimental population analysis of $(NH_3)_nNH_4^+$ ($n = 0-18$) and $(NH_3)_nNH_2^-$ ($n = 0-8$) cluster series show a special stability at $n = 4$ and 16 and $n = 2$, 4, and 6, respectively.

DFT/B3LYP calculations of the $(NH_3)_{0-8}NH_4^+$ clusters showed that the structures of the more stable conformers follow a clear pattern: each additional NH_3 group makes a new hydrogen bond with one of the hydrogen atoms of an NH_3 unit already bound to the NH_4^+ core. For the $(NH_3)_{0-8}NH_2^-$ clusters, the DFT/B3LYP calculations showed that, within the calculation error, the more stable conformers follow a clear pattern for $n = 1-6$: each additional NH_3 group makes a new hydrogen bond to the NH_2^- core. For $n = 7$ and 8, the additional NH_3 groups bind to other NH_3 groups, probably because of the saturation of the NH_2^- core.

A stability analysis was performed using the commonly defined stability function $E_{n-1} + E_{n+1} - 2E_n$, where E is the total energy of the cluster, including the zero point correction energy ($E = E_t + \mathrm{ZPE}$). The trend on the relative stability of the clusters presents an excellent agreement with the distribution of experimental cluster abundances. Moreover, the stability analysis predicts that $(NH_3)_4NH_4^+$ and the even negative clusters [$(NH_3)_nNH_2^-$, $n = 2$, 4, and 6] should be the most stable ones, in perfect agreement with the experimental results.

On the basis of the differences of binding energies among the neutral and charged clusters, it is suggested that, since the forces holding the NH_3 units together in the charged clusters are stronger than those in the neutral ones, the clustering process from ice bombardment should start with the addition of neutral NH_3 units to charged fragments preferentially to the addition of small charged fragments to neutral $(NH_3)_n$ clusters.

Acknowledgment. The authors acknowledge the Brazilian Agencies CNPq, Faperj, and CLAF for their support.

References and Notes

(1) Castleman, A. W.; Bowen, K. H. *J. Phys. Chem.* **1996**, *100*, 12911.
(2) Farrar, J. M. In *Current Topics in Ion Chemistry and Physics*; Ng, C. Y., Powis, I., Eds.; Wiley: New York, 1992.
(3) Johnson, M. A.; Lineberger, W. C. In *Techniques for the Study of Ion Molecule Reactions*; Farrar, J. M., Saunders, W. H., Eds.; Wiley: New York, 1988; p 591.
(4) Castleman, A. W., Jr. In *Clusters of Atoms and Molecules*; Haberland, H., Ed.; Springer-Verlag: New York, 1992.
(5) Johnston, R. L. *Atomic and Molecular Clusters*; Taylor & Francis: London, 2002.
(6) Sugano, S. *Microcluster Physics*; Springer-Verlag: Berlin, 1991.
(7) Kryachko, E. S. *Chem. Phys. Lett.* **1997**, *272*, 132.
(8) Kim, J.; Majumbar, D.; Lee, H. M.; Kim, K. S. *J. Chem. Phys.* **1999**, *110*, 9128.
(9) Sadlej, J.; Kzimirski, J. K.; Buck, U. *J. Phys. Chem. A* **1999**, *103*, 9128.
(10) Smith, D. M.; Smets, J.; Elkadi, A.; Adamowics, L. *J. Chem. Phys.* **1998**, *109*, 1238.
(11) Kulkarni, S. A.; Bartolotti, L. J.; Pathak, R. K. *J. Chem. Phys.* **2000**, *113*, 2697.
(12) Pawlowski, P. M.; Okimoto, S. R.; Tao, F. M. *J. Phys. Chem. A* **2003**, *107*, 5327.
(13) Antolovich, M.; Lindoy, L. F.; Reimers, J. R. *J. Phys. Chem. A* **2004**, *108*, 8434.

(14) Sadlej, J.; Moszynski, M.; Doborowolski, J. Cz.; Mazurek, A. P. *J. Phys. Chem. A* **1999**, *103*, 8529.
(15) Armunanto, R.; Schwenk, C. F.; Rode, B. M. *J. Phys. Chem. A* **2005**, *109*, 4437.
(16) Lenz, A.; Ojamae, L. *Phys. Chem. Chem. Phys.* **2005**, *7*, 1905.
(17) Schulz, F.; Hartke, B. *Phys. Chem. Chem. Phys.* **2003**, *5*, 5021.
(18) Sobolewski, A. L.; Domcke, W. *Phys. Chem. Chem. Phys.* **2005**, *7*, 970.
(19) Farenzena, L. S.; Martinez, R.; Iza, P.; Ponciano, C. R.; Homen, M. G. P.; Naves de Brito, A.; da Silveira, E. F.; Wien, K. *Int. J. Mass Spectrom.* **2006**, *255*, 1.
(20) Odutola, J. A.; Dyke, T. R.; Howard, B.; Muether, J. S. *J. Chem. Phys.* **1979**, *70*, 4884.
(21) Süzer, S.; Andrews, L. *J. Chem. Phys.* **1987**, *87*, 5131.
(22) Wei, S.; Kilgore, K.; Tzeng, W. B.; Castleman, A. W., Jr. *J. Chem. Phys.* **1990**, *92*, 332.
(23) Wei, S.; Kilgore, K.; Tzeng, W. B.; Castleman, A. W., Jr. *J. Chem Phys.* **1990**, *93*, 2506.
(24) Wei, S.; Kilgore, K.; Tzeng, W. B.; Castleman, A. W., Jr. *J. Phys. Chem.* **1991**, *95*, 8306.
(25) Shinohara, H.; Nishi, N.; Washida, N. *J. Chem. Phys.* **1985**, *83*, 1939.
(26) Peifer, W. R.; Coolbaugh, M. T.; Garvey, J. F. *J. Chem. Phys.* **1989**, *91*, 6684.
(27) Lifshitz, C.; Louage, F. *J. Phys. Chem.* **1989**, *93*, 5635.
(28) Ichihashi, M.; Yamabe, J. Y.; Muray, K.; Nonose, S.; Hirao, K.; Kondow, T. *J. Phys. Chem.* **1996**, *100*, 10050.
(29) Card, D. A.; Folmer, D. E.; Sato, S.; Buzza, S. A.; Castleman, A. W., Jr. *J. Phys. Chem. A* **1997**, *101*, 3417.
(30) Freudenberg, Th.; Stert, V.; Radloff, W.; Ringling, J.; Güddle, J.; Korn, G.; Hertel, V. *Chem. Phys. Lett.* **1997**, *269*, 523.
(31) Wei, S.; Purnell, J.; Buzza, S. A.; Stanley, R. J.; Castleman, A. W., Jr. *J. Chem. Phys.* **1992**, *97*, 9480.
(32) Snodgrass, J. T.; Coe, J. V.; Freidhoff, C. B.; McHugh, K. M.; Arnold, S. T.; Bowen, K. H. *J. Phys. Chem.* **1995**, *99*, 9675.
(33) Martinez, R.; Ponciano, C. R.; Farenzena, L. S.; Iza, P.; Homen, M. G. P.; Naves de Brito, A.; Wien, K.; da Silveira, E. F. *Int. J. Mass Spectrom.* **2006**, *253*, 112.
(34) Farenzena, L. S.; Iza, P.; Martinez, R.; Fernandez-Lima, F. A.; Seperuelo, E. D.; Faraudo, G. S.; Ponciano, C. R.; Homem, M. G. P.; Naves de Brito, A.; Wien, K.; da Silveira, E. F. *Earth, Moon, Planets*, in press.
(35) Farenzena, L. S.; Collado, V. M.; Ponciano, C. R.; da Silveira, E. F.; Wien, K. *Int. J. Mass Spectrom.* **2005**, *243*, 85.
(36) Wien, K.; de Castro, C. S. C. *Nucl. Instrum. Methods B* **1989**, *146*, 178.
(37) Collado, V. M.; Farenzena, L. S.; Ponciano, C. R.; da Silveira, E. F.; Wien, K. *Surf. Sci.* **2004**, *569*, 149.
(38) Betts, R. L.; da Silveira, E. F.; Schweikert, E. A. *Int. J. Mass Spectrom.* **1995**, *145*, 9.
(39) Johnson, R. E. *Energetic Charged Particles Interaction with Atmospheres and Surfaces*; Springer-Verlag: Heidelberg, 1990.
(40) Woon, D. E. *Icarus* **2001**, *149*, 277.
(41) Lorenz, R. D.; Lunine, J. I. *Icarus* **1996**, *122*, 79.
(42) Engelking, P. C. *J. Chem. Phys.* **1986**, *85*, 3103.
(43) Stace, A. J. *J. Chem. Phys.* **1986**, *85*, 5774.
(44) Klots, C. E. *J. Chem. Phys.* **1985**, *83*, 5854.
(45) Klots, C. E. In *The Wiley Series in Ion Chemistry and Physics: Cluster Ions*; Bauer, T., Ng, C. Y., Powis, I., Eds.; Wiley: New York, 1994.
(46) Pullman, A.; Armbruster, A. M. *Chem. Phys. Lett.* **1975**, *36*, 558.
(47) Hirao, K.; Fujikawa, T.; Konishi, H.; Yamabe, S. *Chem. Phys. Lett.* **1984**, *104*, 184.
(48) Nakai, H.; Goto, T.; Ichikawa, T.; Okada, Y.; Orii, T.; Takeuchi, K. *Chem. Phys.* **2000**, *262*, 201.
(49) Demaison, J.; Margules, L.; Boggs, J. E. *Chem. Phys.* **2000**, *260*, 65.
(50) Daigoku, K.; Miura, N.; Hashimoto, K. *Chem. Phys. Lett.* **2001**, *346*, 81.
(51) Wang, B. C.; Chang, J. C.; Jiang, J. C.; Lin, S. H. *Chem. Phys.* **2002**, *276*, 93.
(52) Martin, J. M. L.; Lee, T. J. *Chem. Phys. Lett.* **1999**, *258*, 129.
(53) McFarlane, R. D.; Torgerson, D. F. *Phys. Rev. Lett.* **1976**, *36*, 486.
(54) *Jaguar 5.5 and Jaguar 6.0*; Schroedinger Inc.: Portland, OR, 2004.
(55) Rosch, N.; Trickey, S. B. *J. Chem. Phys.* **1997**, *106*, 8940.
(56) Crofton, M. W.; Price, J. M.; Yee, Y. T. IR spectroscopy of hydrogen bonded charged clusters. In *Clusters of Atoms and Molecules*; Haberland, H., Ed.; Springer-Verlag: Berlin, 1994; Vol. II.
(57) de Castro, C. C.; Bitensky, I. S.; da Silveira, E. F. *Nucl. Instrum. Methods B* **1997**, *132*, 561.
(58) Breneman, C. M.; Wiberg, K. W. *J. Comput. Chem.* **1990**, *11*, 361.
(59) Kulkarni, S. A.; Pathak, R. K. *Chem. Phys. Lett.* **2001**, *336*, 278.